THE JOURNAL OF PHYSICAL CHEMISTRY Letters

LETTER

pubs.acs.org/JPCL

Time- and Polarization-Resolved Photoluminescence of Individual Semicrystalline Polythiophene (P3HT) Nanoparticles

Joelle A. Labastide,[†] Mina Baghgar,[‡] Irene Dujovne,[†] B. Harihara Venkatraman,[†] David C. Ramsdell,[†,§] Dhandapani Venkataraman,[*,†] and Michael D. Barnes[*,†,‡]

[†]Department of Chemistry and [‡]Department of Physics, University of Massachusetts Amherst, 710 North Pleasant Street, Amherst, Massachusetts 01003, United States

Supporting Information

ABSTRACT: We report on a remarkable size and internal structure dependence on time- and polarization-resolved photoluminescence (PL) from individual regioregular rrP3HT (poly-3-(hexylthiophine)) nanoparticles. For the smallest particles (~34 nm) with relatively low crystallinity (40%), the time evolution of polarization contrast is nearly stationary; for intermediate-sized particles (~ 65 nm), depolarization occurs on a 1−2 ns time scale. The largest and most crystalline particles studied (118 nm, 70%) show a PL depolarization on a time scale of <50 ps. In every time regime, we observe P3HT nanoparticle PL dynamics that are qualitatively different from those of extended films and single-polymer chains, highlighted by intriguing differences in power law dynamics in the PL intensity at long times. This work may support the hypothesis that hierarchical assemblies of conducting polymer nanoparticles could offer a route to higher efficiency in organic photovoltaic systems.

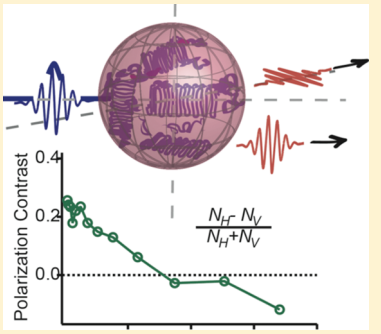

SECTION: Nanoparticles and Nanostructures

The problem of short characteristic exciton diffusion lengths (~10−15 nm) in organic semiconductors has generated significant interest in nanostructured assemblies of conjugated polymers for solar energy harvesting applications. Directed assembly of p-/n-type semiconducting polymer nanoparticles offers an interesting possible solution to the mesoscale morphology problem in organic light harvesting systems, where both dimensions and stable packing geometries may give rise to more robust and efficient organic PV devices.[1a−e] Recent studies by several groups point to the importance of control over particle size and internal structural order for the optimization of charge efficiency and charge separation.[1c,d,2] The interesting aspect of the nanoparticle approach for photovoltaic applications is that for certain nanoparticle packing structures that can, in principle, be defined by nanoparticle size, there exist extended, continuous, conducting paths for electrons and holes. In keeping with this thinking, the Venkatraman group has devised new synthetic methodologies for preparing nanoparticles of organic semiconductors with tunable sizes and degrees of crystallinity. In this Letter, we examine the time- and polarization-resolved photoluminescence (PL) from individual regioregular rr-P3HT (poly-3-(hexylthiophine)) nanoparticles as a function of both size and internal crystallinity (unpublished results). Our measurements reveal PL dynamics that depend on both size and internal structure, and that are qualitatively different from extended P3HT films in every decay time regime. Perhaps most interesting is the observed size dependence in the long-time regime, which, when described with a power law decay (related to mean electron−hole separation distances), shows significantly larger exponent values than those recently observed in extended films.[3] These results yield new understanding of the relationship between photophysics and nanoparticle properties and imply the feasibility of hierarchical assemblies of conducting polymer nanoparticles[4] as a route to higher efficiency in organic PV systems.

The photophysics of polythiophene and polythiophene blends are currently the focus of intense research efforts across many different disciplines. Recent studies of time-resolved pump−probe polarization anisotropy in absorption and luminescence[5] using fluorescence upconversion[6] and streak camera techniques[3,7] have been reported for P3HT in thin films, pointing to exciton migration and charge separation processes that occur on time scales on the order of a few picoseconds,[6a] as well as long time scale dynamics attributed to radiative recombination of polaron pairs.[3,8] However, because of the sensitivity to path length and absorber density in ultrafast methods, such techniques are difficult to apply to single molecules or isolated nanostructures. Polarization methods, in particular, are powerful tools for elucidating the details of internal order and multichromophoric character in single-polymer chains and nanoparticles.[4,9a−9e] However, such "steady-state" polarization methods are incapable of recovering dynamical information from single molecules or isolated nanostructures on time scales shorter

Received: July 13, 2011
Accepted: August 1, 2011
Published: August 01, 2011

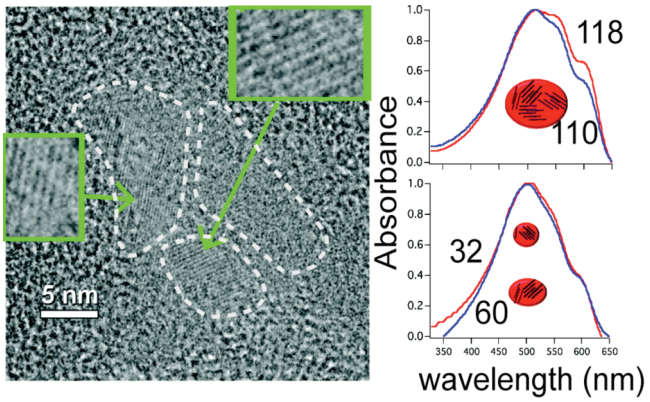

Figure 1. (Left) HRTEM image of a 116 nm particle. Crystalline domains of about 5−10 nm have been highlighted. The insets display the crystalline arrangements of each crystal. From these images, it is evident that the internal crystalline domains are randomly oriented. (Right) Normalized UV−vis absorption of four nanoparticle families. (Bottom) Two of these nanoparticles have different mean sizes (32 and 60 nm as determined from DLS) and the same crystallinity, as determined by the UV−vis absorption, while (Top) we display UV−vis absorption for two families of similar size but different crystalinity, as evident from the difference in the shoulder at 600 nm.

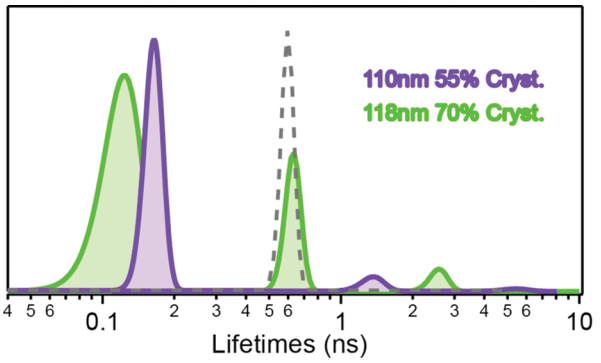

Figure 2. Gaussian fits of histograms of PL decay components from P3HT nanoparticles: 118 nm, 70% crystalline and 115 nm, 55% crystalline. Histogram areas have been normalized to show the relative contributions (amplitudes) of each decay component. The distribution of single-exponential decay times for single P3HT chains of $\langle\tau\rangle = 600$ ps is shown by the dashed curve (arbitrary scale).

than ∼1 μs due to limitations imposed by mechanical rotation times or CCD camera frame rates.

Figure 1 summarizes the properties of the P3HT nanoparticles under investigation here. The ratio between the intensities of the vibronic band (610 nm) and the main absorption band in the UV/vis absorption spectra of aqueous dispersions of nanoparticles provided a measure of net crystallinity. High-resolution transmission electron microscopy (HRTEM) images confirm the semicrystalline nature of the nanoparticles and provide the additional insight that the particles are actually polycrystalline, with multiple crystalline domains that are nonuniformly oriented. The nominal sizes of the nanoparticle families were determined with dynamic light scattering (DLS) and confirmed with AFM surface height scans.

The experiments described here employ a variant of time-tagged/time-resolved (T3R) single-photon counting, with access to polarization dynamics on time scales ultimately limited by the (picosecond) time-to-digital conversion resolution. We used a pair of high-timing precision avalanche photodiodes (APDs) (id Quantique id100−50) arranged in a Hanbury−Brown Twiss configuration and registered to the same point in the sample plane. This point corresponds to the center of an iris that was placed in the emission path and tightened so that the fluorescence signal of only a single particle would be sent through the detection path. This, along with sparse particle populations in the sample plane (described in Supporting Information), ensured that all signals collected were from single particles. A neutral 50/50 beamsplitter was used to divide the fluorescence signal, followed by linear analyzers in front of each APD to sort signal photons by polarization state (perpendicular/parallel) with respect to the polarization of the excitation pulse. The individual APD signals were input into a precision channel router (PicoQuant PHR800 Uni-Router) and directed into a time-to-digital converter (PicoQuant TimeHarp300_V2) operating in T3R mode. As in conventional T3R measurements,[10] this approach enables construction of fluorescence lifetime trajectories by sorting a cluster of photon events within a given *global* time segment by (*local*) arrival time relative to the most recent excitation pulse. Because each detected photon has an additional polarization "tag", we have access to information on the picosecond time evolution of the polarization contrast, as well as polarization correlations between individual photon detection events.

We used a vertically polarized PicoQuant pulsed diode laser operating at 440 nm (pulse width ≈ 50 ps) with a 10 or 40 MHz repetition rate as an excitation source. The laser spot was weakly focused (∼10 μm spot size) and set up in epi-illumination geometry, with an average nominal input intensity of ∼1 kW/cm^2. Nanoparticle sizes were determined using both dynamic light scattering (DLS) and in situ AFM surface height measurements. Isolated P3HT nanoparticle samples were prepared by drop-casting from dilute (∼10^{-9} M) aqueous solution onto plasma-cleaned glass coverslips. PL data from individual particles were accumulated for typically 3−5 min. Detailed count rate analysis (Supporting Information) of the PL from different nanoparticle families showed the onset of a process that competes with radiative recombination and that scales with the particle size and internal volume fraction of crystalline P3HT. This could be a similar effect as that observed for collapsed MEH-PPV chains by the Scheblykin group.[11]

Figure 2 summarizes the PL decay distributions from two different NP families, 115 nm (55% crystallinity), and 118 nm (70% crystallinity). Each single-particle decay function was fit to a decaying three-exponential function convoluted with our instrument response function (see Supporting Information for details). The peaks in Figure 2 are Gaussian fits to histograms of decay constants, whose areas have been scaled according to the relative contribution to the total detected PL, thus approximating a decay rate probability function. The dashed gray curve represents the distribution of single-exponential decay constants obtained from single chains of P3HT cast from chloroform. Thus, the central peak, which appears between 300 and 900 ps depending on particle size, is associated with radiative decay of the relaxed singlet exciton,[6a] although it presents with considerable variability among the different nanoparticle families (data not shown). The long-time decay components that appear above 500 ps are most sensitive to the crystallinity− an effect that is most prominent in the largest nanoparticle family with the highest crystallinity.

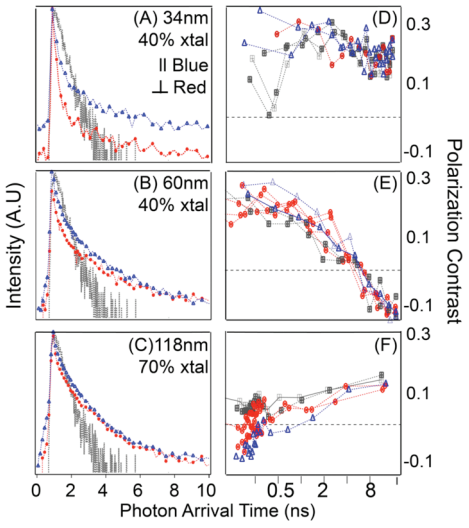

Figure 3. Polarization-resolved PL decay from different P3HT nanoparticles, (A) 34 nm/40%xtal, (B) 60 nm/40%xtal, and (C) 118 nm/70%xtal. The corresponding polarization contrast parameter time evolution for (A−C) is given in (D−F). The scale for the polarization contrast, *M*, is the same for all (D−F), and the time-resolved count data have been segmented to give approximately equal numbers of total counts at each time. The different traces in (D−F) correspond to different time segments in the PL trajectory.

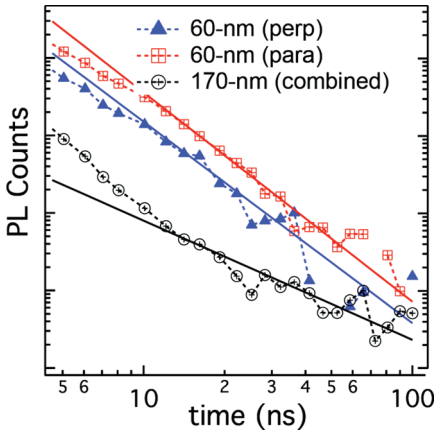

Figure 4. Power law analysis of long-time PL decay from 60 nm (blue triangles and red squares denote different polarization components) and 170 nm (gray circles, polarization contributions combined) P3HT nanoparticles. Signals from ∼20 different particles within the same size family were combined. The data were binned at 5 ns intervals between 20 and 100 ns. The red and blue solid lines represent fits to the PL data with a power law argument of μ = 1.7; the solid black line indicates a power law fit with μ = 0.7 (±0.1).

Figure 3A−C displays polarization-resolved PL decay data for 34 and 60 nm (both with 40% crystallinity) and 118 nm (70% crystallinity) NPs, compared with the (single-exponential) PL decay of a single P3HT chain (gray trace). Figure 3D−F shows the corresponding polarization contrast, $M = (N_{para} - N_{perp})/(N_{para} + N_{perp})$; $N_{para/perp}$ are the number of detected counts in the parallel/perpendicular polarization channels as a function of local photon arrival time (ns). In this analysis, the *local* photon arrival times (relative times referenced to the excitation pulse) were binned to give approximately equal numbers of counts in each local time segment, thus roughly equal in uncertainty in *M*. For the 34 nm sample, the polarization contrast appears nearly stationary in local time, with a typical mean value of $M = 0.25$. For the largest particles, the PL appears to be almost completely depolarized at early times and acquires a weak (positive) bias at longer times. By far the most interesting behavior is seen for the 60 nm NPs, which show PL depolarization on a 1−2 ns time scale. In every particle family studied, the time variation of polarization contrast with local time appears roughly independent of which global time segment is selected in the PL trajectory. Thus, the underlying dynamics governing the time evolution of polarization contrast seem to be constant in coarse time and only weakly associated with photobleaching. We speculate that the size dependence in the time evolution of polarization contrast could be due to the relationship between crystal domain sizes and the number of different crystalline domains within each nanoparticle. Preliminary HRTEM results (Figure 1) show that the largest particles with the largest percent crystallinity are polycrystalline, with crystal domains that are on the order of 10 nm. If the average initial crystalline domain size is independent of nanoparticle size (that is, formed prior to nanoparticle assembly), then size constraints allow for only two or three crystalline domains in the smallest particles, thus producing strong (and constant) polarization anisotropies. In contrast, the largest polycrystalline particles would presumably have randomly oriented domains, thereby giving depolarized emission at short time scales.

Recent reports[3] have suggested that radiative recombination in P3HT occurs primarily at the interface of lamellar (crystalline) and poorly stacked (amorphous) domains.[3,12a,12b] Charge separation occurs over subnanosecond time scales (thus scrambling the polarization in emission) by dissociation of excitons created at interfaces between lamellar (aggregate) and poorly stacked (nonaggregate) domains. Thus, the time evolution of the polarization contrast that we observe in the 34 and 60 nm nanoparticles could be related to anisotropic exciton diffusion within the crystal domain directions. The distinct time evolution in the 60 nm particle family may be a consequence of a crystal "ripening" effect. In smaller particles, surface energy and size constraints would inhibit further growth of crystalline domains through nucleation. Because the nanoparticles with the highest crystallinity are likely highly polycrystalline, there may be numerous nucleation sites, which would mean that the average individual domain size would not change very much through nucleated crystal growth. The 60 nm particle with low crystallinity may have the proper conditions for significant nucleated crystal growth, and therefore, the crystal domains may be larger than those in the small and large, but polycrystalline, particles.

In the model proposed recently by Paquin and co-workers to describe the time dependence of PL decay in P3HT films,[3] the long-time dynamics can be modeled with a power law, given by $I(t) \approx A \cdot t^{-(1+\mu)}$, where *A* is an amplitude and the power law exponent μ is given by the ratio of the mean e^-/h^+ radius and a distance parameter characterizing tunneling in the material.[3,8b] Paquin and co-workers reported a value of μ = 0.54 for neat P3HT films, which appeared to be independent of temperature and polarization. Figure 4 shows a comparison of PL decay in the long-time regime from 60 and 170 nm P3HT nanoparticles with 40 and 50% crystallinity, respectively. Because the PL is so weak in this time regime at room temperature, PL decay signals from approximately 20 different nanoparticles, collected individually, within a particular family were combined for the analysis. For the

dx.doi.org/10.1021/jz200958x |*J. Phys. Chem. Lett.* 2011, 2, 2089–2093

170 nm sample, we recovered a value of $\mu = 0.7 \pm 0.1$, which is close to the reported thin film value.[3] For the 60 nm sample, we obtained a value of $\mu = 1.7$ (± 0.1), nearly a factor of 3 larger than the thin film value. This suggests that the average electron−hole radius is significantly larger in the 60 nm particles. This could be due in part to screened electrostatic interactions between carriers inside the nanoparticle and charges on the surfactant bound to the surface. Alternatively, a reduction of the charge tunneling distance in the material due to confinement in the nanoparticles could also increase the value of the power law exponent. The larger power law exponent for the PL decay in 60 nm particles may, as we speculated earlier, be associated with larger crystalline domain sizes.

In summary, our measurements of polarization- and time-resolved photoluminescence from P3HT nanoparticles have revealed an interesting dependence on particle size and internal structure. Qualitatively, these results can be interpreted in terms of an enhanced probability of charge separation upon photoexcitation that competes with radiative recombination and increases with increasing internal P3HT nanoparticle crystal fraction. This interpretation is supported by the PL intensity and count rate data, which shows a dramatic falloff (compared with a simple r^3 dependence) with particle size, (shown in Supporting Information). In addition, the time evolution of polarization contrast indicates an interesting size/structure-dependent polarization dephasing; the origin of this is not completely clear. Finally, the power law analysis of the long-time PL decay suggests a significantly larger mean electron−hole radius for smaller nanoparticles, which may facilitate higher charge harvesting efficiencies in a nanoparticle-based organic photovoltaic architecture.

■ ASSOCIATED CONTENT

Supporting Information. Details of data collection, analysis, and sample preparation. This material is available free of charge via the Internet at http://pubs.acs.org.

■ AUTHOR INFORMATION

Corresponding Author

*E-mail: DV@chem.umass.edu (D.V.); mdbarnes@chem.umass.edu (M.D.B.).

Present Addresses

[§]Department of Chemistry, University of Maryland—College Park.

■ ACKNOWLEDGMENT

This material is based on work supported as part of Polymer-Based Materials for Harvesting Solar Energy, an Energy Frontier Research Center funded by the U.S. Department of Energy, Office of Science, Office of Basic Energy Sciences, under Award Number DE-SC0001087. J.A.L. acknowledges a NEAGEP fellowship under the support of NSF Grant S21000025700000. M.D.B. acknowledges support of the U.S. Department of Energy Basic Energy Sciences (DE-FG02-05ER15965). The assistance of Dr. Doug Wei, Zeiss Instruments, Inc., for the HRTEM imaging is gratefully acknowledged.

■ REFERENCES

(1) (a) Wang, H.; Wang, H. Y.; Gao, B. R.; Wang, L.; Yang, Z. Y.; Du, X. B.; Chen, Q. D.; Song, J. F.; Sun, H. B. Exciton Diffusion and Charge Transfer Dynamics in Nano Phase-Separated P3HT/PCBM Blend Films. *Nanoscale* **2011**, *3*, 2280–2285. (b) Drori, T.; Holt, J.; Vardeny, Z. V. Optical Studies of the Charge Transfer Complex in Polythiophene/Fullerene Blends for Organic Photovoltaic Applications. *Phys. Rev. B* **2010**, *82*, 075207. (c) Venkataraman, D.; Yurt, S.; Venkatraman, B. H.; Gavvalapalli, N. Role of Molecular Architecture in Organic Photovoltaic Cells. *J. Phys. Chem. Lett.* **2010**, *1*, 947–958. (d) Hu, Z. J.; Tenery, D.; Bonner, M. S.; Gesquiere, A. J. Correlation between Spectroscopic and Morphological Properties of Composite P3HT/PCBM Nanoparticles Studied by Single Particle Spectroscopy. *J. Lumin.* **2010**, *130*, 771–780. (e) Millstone, J. E.; Kavulak, D. F. J.; Woo, C. H.; Holcombe, T. W.; Westling, E. J.; Briseno, A. L.; Toney, M. F.; Frechet, J. M. J. Synthesis, Properties, and Electronic Applications of Size-Controlled Poly(3-hexylthiophene) Nanoparticles. *Langmuir* **2010**, *26*, 13056–13061.

(2) (a) Gao, Y. Q.; Martin, T. P.; Thomas, A. K.; Grey, J. K. Resonance Raman Spectroscopic and Photocurrent Imaging of Polythiophene/Fullerene Solar Cells. *J. Phys. Chem. Lett.* **2010**, *1*, 178–182. (b) Dante, M.; Peet, J.; Nguyen, T. Q. Nanoscale Charge Transport and Internal Structure of Bulk Heterojunction Conjugated Polymer/Fullerene Solar Cells by Scanning Probe Microscopy. *J. Phys. Chem. C* **2008**, *112*, 7241–7249. (c) Marsh, R. A.; Hodgkiss, J. M.; Albert-Seifried, S.; Friend, R. H. Effect of Annealing on P3HT:PCBM Charge Transfer and Nanoscale Morphology Probed by Ultrafast Spectroscopy. *Nano Lett.* **2010**, *10*, 923–930. (d) Lin, H. Z.; Hania, R. P.; Bloem, R.; Mirzov, O.; Thomsson, D.; Scheblykin, I. G. Single Chain versus Single Aggregate Spectroscopy of Conjugated Polymers. Where Is the Border? *Phys. Chem. Chem. Phys.* **2010**, *12*, 11770–11777. (e) Tuncel, D.; Demir, H. V. Conjugated Polymer Nanoparticles. *Nanoscale* **2010**, *2*, 484. (f) Pecher, J.; Mecking, S. Nanoparticles of Conjugated Polymers. *Chem. Rev.* **2010**, *110*, 6260–6279. (g) Kietzke, T.; Neher, D.; Landfester, K.; Montenegro, R.; Güntner, R.; Scherf, U. Novel Approaches to Polymer Blends Based on Polymer Nanoparticles. *Nat. Mater.* **2003**, *2*, 408–412.

(3) Paquin, F.; Latini, G.; Sakowicz, M.; Karsenti, P.-L.; Wang, L.; Beljonne, D.; Stingelin, N.; Silva, C. Charge Separation in Semicrystalline Polymeric Semiconductors by Photoexcitation: Is the Mechanism Intrinsic or Extrinsic? *Phys. Rev. Lett.* **2011**, *106*, 197401.

(4) Hassey, R.; McCarthy, K. D.; Basak, E. S. D.; Venkataraman, D.; Barnes, M. D. Single-Molecule Chiroptical Spectroscopy: Fluorescence Excitation of Individual Helicene Molecules in Polymer-Supported Thin-Films. *Chirality* **2008**, *20*, 1039–1046.

(5) (a) Xie, Y.; Li, Y.; Xiao, L. X.; Qiao, Q. Q.; Dhakal, R.; Zhang, Z. L.; Gong, Q. H.; Galipeau, D.; Yan, X. Z. Femtosecond Time-Resolved Fluorescence Study of P3HT/PCBM Blend Films. *J. Phys. Chem. C* **2010**, *114*, 14590–14600. (b) Banerji, N.; Cowan, S.; Leclerc, M.; Vauthey, E.; Heeger, A. J. Exciton Formation, Relaxation, and Decay in PCDTBT. *J. Am. Chem. Soc.* **2010**, *132*, 17459–17470. (c) Parkinson, P.; Muller, C.; Stingelin, N.; Johnston, M. B.; Herz, L. M. Role of Ultrafast Torsional Relaxation in the Emission from Polythiophene Aggregates. *J. Phys. Chem. Lett.* **2010**, *1*, 2788–2792. (d) Piris, J.; Dykstra, T. E.; Bakulin, A. A.; van Loosdrecht, P. H. M.; Knulst, W.; Trinh, M. T.; Schins, J. M.; Siebbeles, L. D. A. Photogeneration and Ultrafast Dynamics of Excitons and Charges in P3HT/PCBM Blends. *J. Phys. Chem. C* **2009**, *113*, 14500–14506.

(6) (a) Banerji, N.; Cowan, S.; Vauthey, E.; Heeger, A. J. Ultrafast Relaxation of the Poly(3-hexylthiophene) Emission Spectrum. *J. Phys. Chem. C* **2011**, *115*, 9726–9739. (b) Trotzky, S.; Hoyer, T.; Tuszynski, W.; Lienau, C.; Parisi, J. Femtosecond up-Conversion Technique for Probing the Charge Transfer in a P3HT:PCBM Blend via Photoluminescence Quenching. *J. Phys. D: Appl. Phys.* **2009**, *42*, 055105.

(7) Westenhoff, S.; Daniel, C.; Friend, R. H.; Silva, C.; Sundstrom, V.; Yartsev, A. Exciton Migration in a Polythiophene: Probing the Spatial and Energy Domain by Line-Dipole Forster-Type Energy Transfer. *J. Chem. Phys.* **2005**, *122*, 094903.

(8) (a) Vardeny, Z. V.; Wei, X. On the Excitonic Nature of the Photoluminescence in Polythiophene Revealed by Odmr Spectroscopy. *Mol. Cryst. Liq. Cryst. Sci. Technol., A* **1994**, *256*, 465–472. (b) Kanner, G. S.; Wei, X.; Hess, B. C.; Chen, L. R.; Vardeny, Z. V. Evolution of Excitons and Polarons in Polythiophene from Femtoseconds to Milliseconds. *Phys. Rev. Lett.* **1992**, *69*, 538–541.

(9) (a) Hu, D. H.; Yu, J.; Wong, K.; Bagchi, B.; Rossky, P. J.; Barbara, P. F. Collapse of Stiff Conjugated Polymers with Chemical Defects into Ordered, Cylindrical Conformations. *Nature* **2000**, *405*, 1030–1033. (b) Barbara, P. F.; Gesquiere, A. J.; Park, S. J.; Lee, Y. J. Single-Molecule Spectroscopy of Conjugated Polymers. *Acc. Chem. Res.* **2005**, *38*, 602–610. (c) Mirzov, O.; Bloem, R.; Hania, P. R.; Thomsson, D.; Lin, H. Z.; Scheblykin, I. G. Polarization Portraits of Single Multichromophoric Systems: Visualizing Conformation and Energy Transfer. *Small* **2009**, *5*, 1877–1888. (d) Mehta, A.; Kumar, P.; Dadmun, M. D.; Zheng, J.; Dickson, R. M.; Thundat, T.; Sumpter, B. G.; Barnes, M. D. Oriented Nanostructures from Single Molecules of a Semiconducting Polymer: Polarization Evidence for Highly Aligned Intramolecular Geometries. *Nano Lett.* **2003**, *3*, 603–607. (e) Cyphersmith, A.; Maksov, A.; Hassey-Paradise, R.; McCarthy, K. D.; Barnes, M. D. Defocused Emission Patterns from Chiral Fluorophores: Application to Chiral Axis Orientation Determination. *J. Phys. Chem. Lett.* **2011**, *2*, 661–665.

(10) Yang, H.; Xie, X. S. Probing Single-Molecule Dynamics Photon by Photon. *J. Chem. Phys.* **2002**, *117*, 10965–10979.

(11) Scheblykin, I. G.; Lin, H. Z.; Tian, Y. X.; Zapadka, K.; Persson, G.; Thomsson, D.; Mirzov, O.; Larsson, P. O.; Widengren, J. Fate of Excitations in Conjugated Polymers: Single-Molecule Spectroscopy Reveals Nonemissive "Dark" Regions in MEH-PPV Individual Chains. *Nano Lett.* **2009**, *9*, 4456–4461.

(12) (a) Spano, F. C.; Clark, J.; Silva, C.; Friend, R. H. Determining Exciton Coherence from the Photoluminescence Spectral Line Shape in Poly(3-hexylthiophene) Thin Films. *J. Chem. Phys.* **2009**, *130*, 074904. (b) Clark, J.; Chang, J. F.; Spano, F. C.; Friend, R. H.; Silva, C. Determining Exciton Bandwidth and Film Microstructure in Polythiophene Films Using Linear Absorption Spectroscopy. *Appl. Phys. Lett.* **2009**, *94*, 16.